Distorted-Wave Born-Approximation Analysis of the $^{42}Ca(p,\alpha)^{39}K$ Reaction Using an Improved Form Factor*

W. R. Falk

Cyclotron Laboratory, Department of Physics, University of Manitoba, Winnipeg, Canada

(Received 18 June 1973)

An improved method of calculating the form factor for the distorted-wave Born-approximation treatment of (p,α) reactions is described that incorporates explicitly the nuclear structure information. The improvement over earlier treatment of the (p,α) reaction is achieved by carrying out a transformation to center-of-mass and internal coordinates of the transferred nucleons, whose individual wave functions are calculated in a Woods-Saxon potential. The formalism is applied to an analysis of the $^{42}Ca(p,\alpha)^{39}K$ reaction performed at a proton bombarding energy of 40.2 MeV. Relative proton spectroscopic factors are deduced for the relatively pure single-hole states at 0.0 ($\frac{3}{2}^+$) and 2.52 ($\frac{1}{2}^+$) MeV in ^{39}K. Good agreement with the proton spectroscopic factors from the $^{40}Ca(d,^3He)^{39}K$ reaction is achieved. The $\frac{5}{2}^+$ states in ^{39}K whose structure is largely unknown contain components important to the (p,α) reaction, but not to the $(d,^3He)$ reaction, as evidenced by their relatively stronger excitation in the (p,α) reaction.

I. INTRODUCTION

Unlike single-nucleon and two-nucleon transfer reactions, more complex direct reactions involving the transfer of three or more nucleons have not, as yet, achieved the status of spectroscopically useful nuclear reactions. However, more and more attention is being paid to such increasingly complicated reactions, as witnessed by numerous recent publications in α-transfer reactions.[1] The hope is that certain simplifying features of these reactions will dominate the observed energy spectra and simple models of the reaction will suffice to yield nuclear structure information. In this paper the direct reaction treatment of the (p, α) reaction is extended through the use of an improved form factor describing the transferred nucleons. Nuclear structure information is incorporated explicitly in this form factor, although due to practical limitations it may frequently be cumbersome to treat this aspect adequately. The analysis presented is applied to the $^{42}Ca(p, \alpha)^{39}K$ reaction and a comparison made to the spectroscopic information obtained from the $^{40}Ca(d, ^3He)^{39}K$ proton pickup reaction.

Many of the special features of the (p, α) reaction have been noted by a number of authors and will be summarized briefly only. These include (i) the coherence[2] in the single-particle states of the three transferred nucleons, (ii) J-dependence,[3,4] and (iii) the ability to reach final nuclei which cannot be investigated by any other pickup reaction.

Some of the early quantitative experimental and theoretical work on the (p, α) reaction was carried out at Princeton by Sherr[5] and Bayman, Brady, and Sherr[6] on $f_{7/2}$-shell nuclei. The main conclusion from their work was that a triton-cluster-pickup description of the reaction adequately accounted for the relative strength of the ground-state cross sections for nuclei of different Z and N. Details of the analysis and results for (p, α) reaction studies on isotopes of copper and zinc have been presented by Nolen.[7]

Fulmer and Ball,[8] treating the (p, α) reaction as the pickup of a proton and a neutron pair, were able to predict the relative intensities of the ground and first-excited-state transitions for the $^{90}Zr(p, \alpha)^{87}Y$ reaction. Good evidence was obtained that pickup is the dominant mechanism to the low-lying states. In this and the preceding distorted-wave Born-approximation (DWBA) analyses a simple radial form factor for the transferred three-nucleon cluster was assumed.

A more detailed analysis of the (p, α) reaction to include finite range effects has been presented by Hird and Li[9] and has been applied to this reaction on targets of ^{19}F, ^{12}C, and ^{27}Al (Refs. 9–11, respectively). Although the deduced spectroscopic factors were within a factor of about 2 of the theoretical values, only the ground-state transition was treated in each case. The radial dependence of the center-of-mass motion of the transferred three-nucleon cluster was obtained by binding a triton in a central potential at the experimental separation energy.

In an attempt to improve the radial form factor used in describing (p, α) reactions Suck and Coker[12] have employed a product of a single-particle proton state with a form factor for the neutrons appropriate to two-nucleon transfer. However, the same radial dependence is used in each of these factors.

Thus among the numerous difficulties and limi-

tations of the DWBA treatment of cluster transfer reactions one of the frequent shortcomings in most treatments is the use of an inadequate form factor. This is the central point to which the present paper addresses itself.

In the following section an expression is derived for the radial form factor of the transferred three-nucleon cluster. Since the over-all objective is the prediction of relative (p, α) cross sections to different excited states, certain factors in the calculation common to all states are frequently not calculated explicitly, but shown only as a normalizing factor.

II. THEORY

A. Wave Function of the Transferred Three-Nucleon Cluster

The treatment of Towner and Hardy[13] for two-nucleon transfer can be extended to the case of three-nucleon transfer. The orbital part of the cluster wave function with orbital angular momentum L and projection M can be written as follows:

$$\phi^{l_1 l_2 l_3}_{M}{}^{L}(\vec{r}_{1B}, \vec{r}_{2B}, \vec{r}_{3B}) = \mathfrak{N} \sum_{\mathfrak{L}'\lambda'} \left\{ \sum_{m_3} (l_3 m_3 \mathfrak{L}'\lambda' | LM) \phi^{n_3 l_3 j_3}_{m_3}(\vec{r}_{3B}) \times \left[\sum_{m_1 m_2} (l_1 m_1 l_2 m_2 | \mathfrak{L}'\lambda') \phi^{n_1 l_1 j_1}_{m_1}(\vec{r}_{1B}) \phi^{n_2 l_2 j_2}_{m_2}(\vec{r}_{2B}) \right] \right\}. \quad (1)$$

Here particle labels 1 and 2 refer to the two neutrons (which are assumed to have their spins coupled to zero) and particle 3 refers to the proton. $\mathfrak{N}$ is a normalization factor arising from the proper antisymmetrization of the over-all three-nucleon wave function and depends on whether or not both neutrons are removed from the same shell.

The single-particle states defined by

$$\phi^{nlj}_{m}(\vec{r}) = (i^l/r) u_{nlj}(r) Y^m_l(\theta, \phi), \quad (2)$$

are calculated in a Woods-Saxon potential well and, to facilitate subsequent mathematical manipulation, the radial parts are expanded in harmonic-oscillator wave functions. Thus,

$$u_{nlj}(r) = \sum_p a_p H_{pl}(\nu r^2). \quad (3)$$

The transformation from the coordinates $\vec{r}_{1B}$, $\vec{r}_{2B}$, and $\vec{r}_{3B}$ to center-of-mass and internal coordinates of the three-nucleon cluster is performed in two steps. Figure 1 illustrates the relevant coordinates. First, the motion of two neutrons is expressed in terms of the coordinates $\vec{R}'$ and $\vec{r}_{12}$. Then, the third particle, the proton, is coupled to the two-neutron cluster yielding an expression in the internal coordinates $\vec{r}_{12}$ and $\vec{r}$, and the center of mass of the three-nucleon cluster, $\vec{R}$. The vector $\vec{r}$ connects the center of mass of the two-neutron pair with the proton. Since the second transformation involves particles of unequal masses, the standard Moshinsky transformation[14, 15] is not applicable. Smirnov[16, 17] has developed methods to handle the general case of coupling particles with arbitrary masses and the method described in his second paper[17] is the one that is employed here. This approach involves expressing the single-particle states in Cartesian coordinates, performing the transformation to relative and center-of-mass coordinates, and then returning to the spherical-coordinate basis. Expressions for the T and A matrices required for this transformation were obtained in closed form and calculated with the computer. The generalized transformation brackets for particles of masses μ_1 and μ_2 are denoted by

$$\left\langle \begin{matrix} p_1 & l_1 & m_1 \\ p_2 & l_2 & m_2 \end{matrix} \middle| \mu_1, \mu_2 \middle| \begin{matrix} N & L & M \\ n & l & m \end{matrix} \right\rangle, \quad (4)$$

where $(p_1 l_1 m_1)$ and $(p_2 l_2 m_2)$ refer to the quantum numbers of the single-particle states, (NLM) the motion of the center of mass of μ_1 and μ_2, and (nlm) the internal motion of the two particles.

Applying this transformation to the combined results of Eqs. (1), (2), and (3), the wave func-

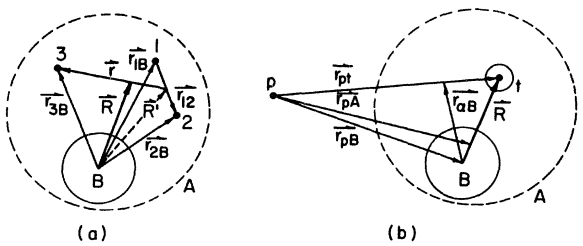

FIG. 1. Representation of the relevant coordinates in the description of the direct $A(p,\alpha)B$ reaction. Particles 1 and 2 refer to the two neutrons and particle 3 to the proton; collectivley these three nucleons are represented by the symbol t (triton).

tion for the three-nucleon cluster becomes:

$$\phi^{l_1 l_2 l_3 L}_M(\vec{R}, \vec{r}_{12}, \vec{r}) = \mathfrak{N} \sum_{\mathcal{L}'\lambda'} \sum_{m_3} \sum_{m_1 m_2} \sum_{p_1 p_2 p_3} i^{l_1+l_2+l_3} a_{p_1} a_{p_2} a_{p_3}$$

$$\times (l_3\, m_3 \mathcal{L}'\, \lambda' | LM)(l_1 m_1 l_2 m_2 | \mathcal{L}'\, \lambda') \sum_{\substack{N'L'M' \\ n'l'm'}} \left\langle \begin{matrix} p_1 & l_1 & m_1 \\ p_2 & l_2 & m_2 \end{matrix} \middle| \mu, \mu \middle| \begin{matrix} N' & L' & M' \\ n' & l' & m' \end{matrix} \right\rangle$$

$$\times \sum_{\substack{N\mathcal{L}\lambda \\ nlm}} \left\langle \begin{matrix} N' & L' & M' \\ p_3 & l_3 & m_3 \end{matrix} \middle| 2\mu, \mu \middle| \begin{matrix} N & \mathcal{L} & \lambda \\ n & l & m \end{matrix} \right\rangle \left[\frac{H_{n'l'}(\nu r_{12}{}^2/2) Y^{m'}_{l'}(\theta_{12}, \phi_{12})}{r_{12}} \right]$$

$$\times \left[\frac{H_{nl}(\frac{2}{3}\nu r^2) Y^m_l(\theta_r, \phi_r)}{r} \right] \left[\frac{H_{N\mathcal{L}}(3\nu R^2) Y^{\lambda}_{\mathcal{L}}(\theta, \phi)}{R} \right]. \tag{5}$$

Energy conservation restricts the above sums as follows:

$$2p_1 + l_1 + 2p_2 + l_2 = 2N' + L' + 2n' + l',$$

$$2N' + L' + 2p_3 + l_3 = 2N + \mathcal{L} + 2n + l,$$

and angular momentum conservation requires that

$$\vec{l}_1 + \vec{l}_2 = \vec{L}' + \vec{l}',$$

$$\vec{L}' + \vec{l}_3 = \vec{\mathcal{L}} + \vec{l}.$$

B. Wave Function of the Target Nucleus

In a treatment of the DWBA analysis of the reaction $A(p, \alpha)B$ it is convenient to expand the target wave function in terms of the wave function of the final nucleus and the transferred nucleons. Again in analogy to the two-nucleon transfer case [Eq. (2.67) of Ref. 13] we write:

$$\phi_{A m_A}^{J_A}(\vec{\xi}_A) = \phi_{A m_A}^{J_A}(\vec{\xi}_B, \vec{r}_{1B}, \vec{r}_{2B}, \vec{r}_{3B})$$

$$= \sum_{[n_1 l_1 j_1][n_2 l_2 j_2][n_3 l_3 j_3]} \, \begin{matrix} L & S & J \\ M & \Sigma & \mathfrak{M} \end{matrix}$$

$$\times \mathcal{G}_{AB}\{[n_1 l_1 j_1][n_2 l_2 j_2][n_3 l_3 j_3]; LSJ\} (J_B m_B J \mathfrak{M} | J_A m_A)(LMS\Sigma | J\mathfrak{M})$$

$$\times \phi_{B m_B}^{J_B}(\vec{\xi}_B) \phi^{l_1 l_2 l_3 L}_M(\vec{R}, \vec{r}_{12}, \vec{r}) \chi^S_\Sigma(1, 2, 3). \tag{6}$$

$\vec{\xi}_B$ represents the coordinates of the B nucleons in the final nucleus and $\chi^S_\Sigma(1, 2, 3)$ is the spin wave function of the three nucleons.

The nuclear structure information is represented through the expansion coefficients $\mathcal{G}_{AB}$ which are the three-nucleon spectroscopic amplitudes. Since, in general, several of these amplitudes may contribute to any given transition, and these are added coherently to obtain the DWBA transition matrix element, a factorization of the nuclear structure information as in single-nucleon transfer is, in general, not possible.

C. DWBA Transition Matrix Element

The transition matrix element in the distorted-wave Born approximation can be written as[18]

$$T_{p\alpha} \equiv T_{p\alpha}(m_p m_A, 0 m_B)$$

$$= \langle \Phi^{(-)}_{\alpha B}(\vec{K}_\alpha, \vec{r}_{\alpha B}) \phi_\alpha \phi_{B m_B}^{J_B} | V_{pA} - \bar{U}_{pA} | \chi^{1/2}_{p m_p} \phi_{A m_A}^{J_A} \Phi^{(+)}_{pA}(\vec{K}_p, \vec{r}_{pA}) \rangle, \tag{7}$$

where $\Phi_{pA}^{(+)}$ and $\Phi_{\alpha B}^{(-)}$ represent the distorted optical-model waves in the incoming and outgoing channel, Φ_α is the α-particle internal wave function, $\chi_{p m_p}^{1/2}$ the incoming proton spin wave function, and ϕ_A and ϕ_B the wave functions for the target and final nucleus, as previously defined. The interaction responsible for the transition—the difference between the sum of the two-body interactions of the proton with the target nucleons and the optical potential $\overline{U}_{pA}$—can be expanded to yield

$$V_{pA} - \overline{U}_{pA} = V_{p1} + V_{p2} + V_{p3} + V_{pB} - \overline{U}_{pA} .$$

Making the usual assumptions that the V_{pB} term largely cancels the $\overline{U}_{pA}$ term, the sum of the last two terms is set equal to zero. With reference to Figs. 1(a) and 1(b), the above interaction can then be expressed as a function of the internal coordinates of the α particle:

$$V_{pA} - \overline{U}_{pA} = V_{\rm int}(\vec{r}_{pt}, \vec{r}_{12}, \vec{r}) .$$

In terms of the coordinates displayed in Fig. 1 the transition matrix element can now be written more explicitly as:

$$\begin{aligned} T_{p\alpha} &\equiv T_{p\alpha}(m_p m_A, 0 m_B) \\ &= \left\langle \Phi_{\alpha B}^{(-)}\left(\vec{K}_\alpha, \vec{R} - \frac{M_p}{M_\alpha}\vec{r}_{pt}\right) \phi_\alpha(\vec{r}_{pt}, \vec{r}_{12}, \vec{r}) \phi_{B m_B}^{J_B}(\vec{\xi}_B) \middle| V_{\rm int}(\vec{r}_{pt}, \vec{r}_{12}, \vec{r}) \right| \\ &\quad \times \chi_{p m_p}^{1/2} \Big\{ \sum^{[n_1 l_1 j_1][n_2 l_2 j_2][n_3 l_3 j_3]} {}_{M\,\Sigma\,\mathfrak{M}}^{L\;S\;J} \vartheta_{AB}([n_1 l_1 j_1][n_2 l_2 j_2][n_3 l_3 j_3]; LSJ) \\ &\quad \times (J_B m_B J \mathfrak{M} | J_A m_A)(LMS\Sigma | J\mathfrak{M}) \phi_{B m_B}^{J_B}(\vec{\xi}_B) \chi_\Sigma^S(1,2,3) \phi^{l_1 l_2 l_3 L}_{\mathfrak{M}}(\vec{R}, \vec{r}_{12}, \vec{r}) \Big\} \left| \Phi_{pA}^{(+)}\left(\vec{K}_p, \vec{r}_{pt} - \frac{M_B}{M_A}\vec{R}\right) \right\rangle . \end{aligned} \tag{8}$$

The integration over the coordinates $\vec{\xi}_B$ of the final nucleus is immediate, but the remaining integrations over the other coordinates can only be performed after further simplification. Here we make the zero-range approximation, writing

$$V_{\rm int}(\vec{r}_{pt}, \vec{r}_{12}, \vec{r}) = D_{p\alpha}^0 \delta(r_{pt}) .$$

Thus, the incoming proton is assumed to interact with the three-nucleon cluster only through its center of mass.

Choosing a simple Gaussian form for the α-particle wave function

$$\phi_\alpha \propto \exp\left(-\eta^2 \sum_{i<j} r_{ij}^2\right),$$

the integral over the internal coordinates appearing in the foregoing expression,

$$I_{nn'} = \int \phi_\alpha(\vec{r}_{pt} = 0, \vec{r}_{12}, \vec{r}) \left[\frac{H_{n'l'}(\nu r_{12}^2/2) Y_{l'}^{m'}(\theta_{12}, \phi_{12})}{r_{12}}\right] \left[\frac{H_{nl}(\frac{2}{3}\nu r^2) Y_l^m(\theta_r, \phi_r)}{r}\right] d\vec{r}_{12}\, d\vec{r}, \tag{9}$$

can be performed. Because of the assumption of relative s-state motion only in the α particle, the above integral is nonzero only for $l = l' = 0$. The result is

$$I_{nn'} \propto I_{nn'}^0 = \left\{\frac{[(2n'+1)!]^{1/2}}{2^{n'} n'!} \frac{(\nu/2)^{3/4}}{\gamma^{3/2}} (1 - 2\nu/\gamma)^{n'}\right\} \left\{\frac{[(2n+1)!]^{1/2}}{2^n n!} \frac{(\frac{2}{3}\nu)^{3/4}}{\Gamma^{3/2}} \left(1 - \frac{3\nu}{2\Gamma}\right)^n\right\}, \tag{10}$$

where

$$\gamma = 8\eta^2 + \nu$$

and

$$\Gamma = 6\eta^2 + \tfrac{3}{4}\nu .$$

The size parameter η of the α particle was taken to be 0.233 fm^{-1} (Ref. 19). Numerical values calculated from expression (10) above show that this integral decreases by about a factor of 3 for each integer increase of the quantity $n + n'$.

Because of the many sums that appear in the expression for the matrix element $T_{p\alpha}$, further simplifications are required to make the calculation tractable. These further simplifications are as follows: (i) $J_A = 0$ (target nucleus spin = 0); (ii) $\vec{l}_1 + \vec{l}_2 = \vec{L}' = 0$ (orbital angular momentum of the two neutrons = 0); and (iii) $\chi_\Sigma^S(1,2,3) = \chi_0^0(1,2)\chi_\epsilon^{1/2}(3)$ (spin of the two neutrons is coupled to zero).

The total angular momentum of the three-nucleon cluster is thus the angular momentum of the proton; the angular momentum transfer in the reaction is hence restricted to the value j_3, and the orbital angular momentum transfer to l_3. Since the sum over l_3 has now vanished we can simplify the three-nucleon spectroscopic amplitude by writing it as a product of a two-nucleon spectroscopic amplitude and a proton spectroscopic factor as follows:

$$\mathcal{G}_{AB}\{[n_1l_1j_1][n_2l_2j_2][n_3l_3j_3],\ LSJ\} = \mathcal{S}^{1/2}(n_3l_3j_3)\mathcal{G}_{AB}\{[n_1l_1j_1][n_2l_2j_2],\ 000\}.$$

The generalized transformation brackets possess the following convenient features:

$$\sum_{m_n}(l_nm_nl_n-m_n|00)\left\langle \begin{matrix} p_1 & l_n & m_n \\ p_2 & l_n & -m_n \end{matrix}\middle|\mu,\mu\middle| \begin{matrix} N' & 0 & 0 \\ n' & 0 & 0 \end{matrix}\right\rangle = (-1)^{l_n}(2l_n+1)^{1/2}\left\langle \begin{matrix} p_1 & l_n & 0 \\ p_2 & l_n & 0 \end{matrix}\middle|\mu,\mu\middle| \begin{matrix} N' & 0 & 0 \\ n' & 0 & 0 \end{matrix}\right\rangle,$$

and

$$\left\langle \begin{matrix} N' & 0 & 0 \\ p_3 & l_3 & m_3 \end{matrix}\middle|2\mu,\mu\middle| \begin{matrix} N & l_3 & m_3 \\ n & 0 & 0 \end{matrix}\right\rangle = \left\langle \begin{matrix} N' & 0 & 0 \\ p_3 & l_3 & 0 \end{matrix}\middle|2\mu,\mu\middle| \begin{matrix} N & l_3 & 0 \\ n & 0 & 0 \end{matrix}\right\rangle;$$

that is, the latter brackets are independent of m_3.

Introducing these simplifications into Eq. (8), the transition matrix element becomes

$$T_{p\alpha} \equiv T_{p\alpha}(m_p 0, 0 m_B) \propto \mathcal{S}^{1/2}(n_3l_3j_3)(J_Bm_BJ_B-m_B|00)(l_3m_p-m_B\tfrac{1}{2}-m_p|J_B-m_B)i^{l_3} \times \int \Phi^{(-)}_{\alpha B}(\vec{K}_\alpha,\vec{R})F(R)Y^{m_p-m_B}_{l_3}(\theta,\phi)\Phi^{(+)}_{pA}\left(\vec{K}_p,-\frac{M_B}{M_A}\vec{R}\right)d\vec{R}, \tag{11}$$

where $F(R)$ is the form factor, given by

$$F(R) = \sum_{p_1p_2p_3N'n'Nn}{}^{[n_1l_nj_1][n_2l_nj_2]}\mathcal{G}_{AB}([n_1l_n\,j_1][n_2l_nj_2];000) \times (2l_n+1)^{1/2}a_{p_1}a_{p_2}a_{p_3}\left\langle \begin{matrix} p_1 & l_n & 0 \\ p_2 & l_n & 0 \end{matrix}\middle|\mu,\mu\middle| \begin{matrix} N' & 0 & 0 \\ n' & 0 & 0 \end{matrix}\right\rangle\left\langle \begin{matrix} N' & 0 & 0 \\ p_3 & l_3 & 0 \end{matrix}\middle|2\mu,\mu\middle| \begin{matrix} N & l_3 & 0 \\ n & 0 & 0 \end{matrix}\right\rangle I_{nn'}\frac{H_{Nl_3}(3\nu R^2)}{R}. \tag{12}$$

The evaluation of the form factor is the major task that has to be carried out before the DWBA cross section can be calculated using standard computer codes.

III. EXPERIMENTAL

The angular distributions for the ^{42}Ca$(p,\alpha)^{39}$K reaction were measured using a 40.2-MeV momentum-analyzed beam from the University of Manitoba sector-focused cyclotron. Two 1-mm surface barrier detectors with an angular separation of 30°, each subtending a solid angle of 1.02×10^{-3} sr, were employed. Since only α paritcles were of interest in the current experiment no particle identification was performed; the ^{42}Ca$(p,{}^3$He$)^{40}$K reaction Q value is −12.65 MeV compared to 0.126 MeV for the ^{42}Ca$(p,\alpha)^{39}$K reaction.

An 825-μg/cm^2 calcium metal foil enriched to $(94.4\pm0.1)\%$ ^{42}Ca was obtained from the Oak Ridge Isotopes Division. The dominant remaining constituent in the target was ^{40}Ca with an abundance of $(5.0\pm0.1)\%$.

The over-all energy resolution in the recorded energy spectra was determined primarily by the energy spread in the incident beam (140 keV) and the energy loss of the α particles in the target (~100 keV). The kinematic spread due to the 0.85° angular acceptance of the detector contributed negligibly compared to the above items. Typical beam currents between 10–20 nA were used in the experiment.

Representative spectra of α particles from the ^{42}Ca$(p,\alpha)^{39}$K reaction are shown in Figs. 2 and 3. Strong excitation is observed for the 0.0-MeV, $\frac{3}{2}^+$, 2.52-MeV, $\frac{1}{2}^+$, 2.81-MeV, $\frac{7}{2}^-$ states, and a group of states at 5.28, 5.62, and 6.52 MeV.

Further strong excitation between channels 700 and 750 is observed. The density of states in ^{39}K is such that levels beyond the 2.81-MeV state are no longer resolved. From the apparent selectivity of the reaction it is possible though that many of these higher peaks in the spectrum are due predominantly to single states. An energy calibration was performed from the known ^{39}K states and the (p,α) reaction on ^{12}C and ^{16}O. Careful account was taken of the energy loss in the ^{42}Ca target and the Mylar calibration target. From this calibration curve each of the labeled particle groups in the spectra was found to represent a well-defined excitation energy in the ^{39}K nucleus when calculated from spectra over a range of

angles. Uncertainty in the assignments of the excitation energies is ±25 keV. The analysis of the spectra to obtain the peak areas was facilitated with a peak-fitting routine.[20] Angular distributions thus deduced are shown in Fig. 4 for the more prominent peaks. The over-all normalization uncertainty in the cross sections is estimated to be ±10%. Only the statistical counting uncertainties are shown in Fig. 4.

IV. STRUCTURE OF ^{39}K

The states strongly excited in the ^{42}Ca(p, α)^{39}K reaction are also, for the most part, the states strongly excited in the ^{40}Ca(d, ^{3}He)^{39}K reaction[21] and the ^{40}Ca(t, α)^{39}K reaction.[22] On the basis of the latter two proton pickup reactions the 0.0-MeV, $\frac{3}{2}^+$ ground state and the 2.52-MeV, $\frac{1}{2}^+$ state in ^{39}K are found to be relatively good hole states in the doubly closed ^{40}Ca core. Lifetime measurements[23] for the 2.52-MeV state support this conclusion, indicating that rather small admixtures of core-coupled configurations could account for the observed lifetime.

Negative-parity states in ^{39}K have been treated theoretically in a conventional shell-model approach by Maripuu and Hokken,[24] in a weak-coupling model by Goode and Zamick,[25] and in an intermediate-coupling model approach by Wiktor.[26] The shell-model calculation indicates a predominantly $(1d_{3/2})^{-2}(1f_{7/2})$ configuration for the 2.81-MeV, $\frac{7}{2}^-$ level. Analysis of experimental $M2$ and $E3$ radiation widths for this level[27] indicate that large collective components in the wave function

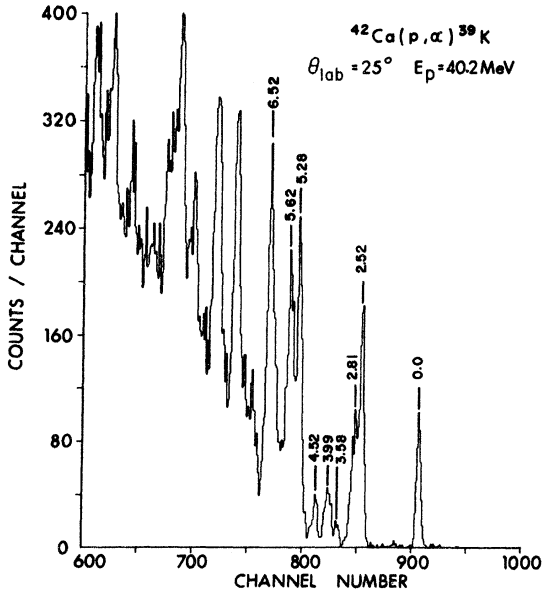

FIG. 2. Energy spectrum of α particles from the ^{42}Ca(p, α)^{39}K reaction at θ_{lab} = 25°.

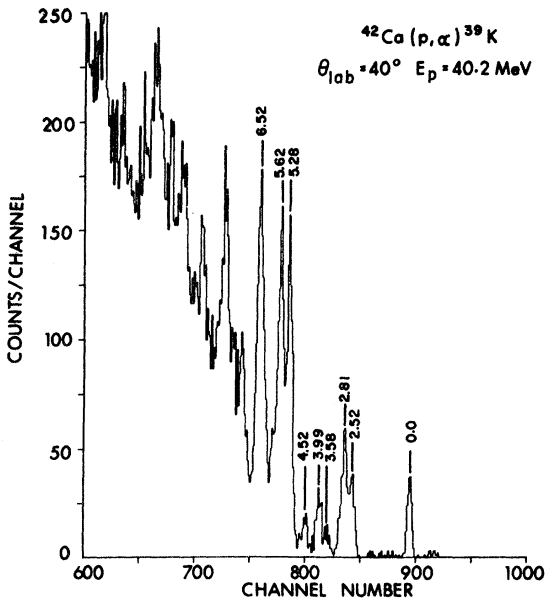

FIG. 3. Energy spectrum of α particles from the ^{42}Ca(p, α)^{39}K reaction at θ_{lab} = 40°.

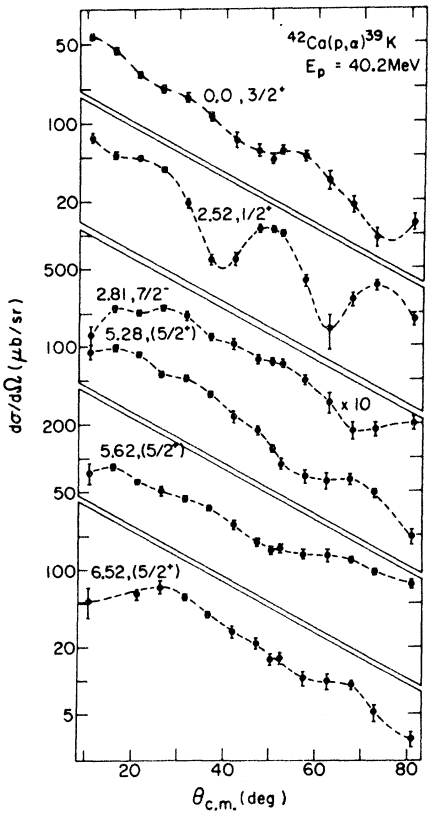

FIG. 4. Experimental angular distributions for states in ^{39}K from the ^{42}Ca(p, α)^{39}K reaction. The dashed curves are lines drawn through the data points to guide the eye. Statistical counting uncertainties only are represented by the error bars.

are not required to explain the experimental results for this state.

What little is known about the higher-lying positive-parity states in ^{39}K has been learned from proton pickup reactions.[21,22] The states observed at 5.28-, 5.62-, and 6.52-MeV excitation energy in ^{39}K in the present (p, α) experiment most likely correspond to the states reported at 5.32, 5.75, and 6.67 MeV by Hiebert, Newman, and Bassel,[21] and those at 5.28, 5.62, and 6.35 MeV by Hinds and Middleton.[22] In these proton pickup reaction studies, characteristic $L=2$ angular distributions were observed for these states which were interpreted as components of the fragmented $1d_{5/2}$ hole state.

In the analysis presented for the ^{42}Ca$(p, \alpha)^{39}$K reaction in this paper only the states alluded to above will be considered, and then within the framework of the relatively simple description discussed above.

V. DWBA ANALYSIS

A. Single-Particle States

The single-particle states required for the generation of the form factor were calculated in a Woods-Saxon potential well with parameters chosen to reproduce closely the experimentally observed single-particle energies. Averaged geometrical parameters from a comprehensive optical-model analysis of ^{40}Ca$+p$ elastic scattering data by van Oers[28] were found to reproduce these single-particle energies rather well, as shown in Fig. 5 and the second column of Table I. A real-well depth of 61.8 MeV was required, and the spin-orbit potential had to be increased to 5.90 from 4.32 MeV in order to obtain the correct spin-orbit splitting between states. These and the remaining optical-model parameters are displayed in the first row of Table III. The experimental single-particle energies of Fig. 5, obtained from binding energies and $(p, 2p)$ reactions, are summarized in papers by Kerman, Svenne, and Villars[29] and Parikh and Svenne.[30]

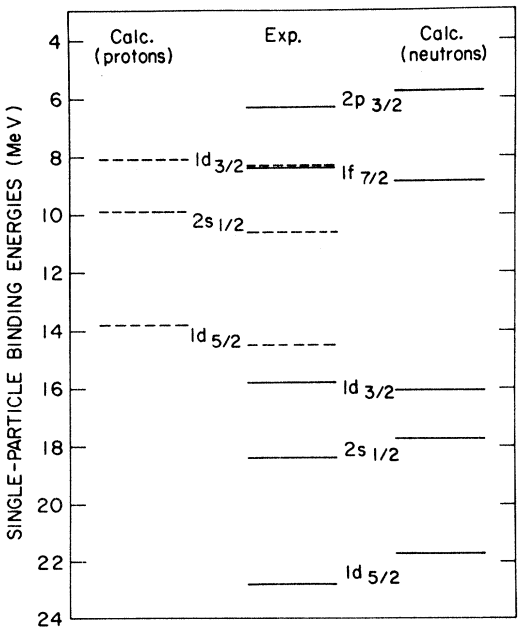

FIG. 5. Comparison of the calculated and experimental single-particle energies for protons and neutrons appropriate to the treatment of the direct ^{42}Ca$(p,\alpha)^{39}$K reaction. Details of the calculation are explained in the text.

The expansion of the single-particle states in harmonic-oscillator functions was limited to three terms only, except for the $2s$ and $2p$ states which could not be adequately represented with fewer than four terms. This limitation was imposed because of the greatly increased number of transformation brackets [see Eq. (5)] required as the number of terms in the expansion was increased. Adequate representation of the single-particle wave functions was obtained up to a radial distance of twice the nuclear radius. Figure 6 shows the results for several representative cases of the neutron and proton single-particle states. The marked deviations observed at distances greater than about 8 fm were found to have negligible effects on the DWBA cross section when the latter was calculated with appropriate modifications to the tail of the form factor.

The harmonic-oscillator expansion coefficients, together with the overlap of this expansion with the single-particle wave functions are given in Table I for the different states. An oscillator parameter of $\nu=0.25$ fm^{-2} was found to give the best average overlap for the given number of terms in the expansion.

An important consideration in particle transfer reactions is the asymptotic form of the wave function of the transferred group of particles. Problems of this nature inherent in two-nucleon transfer reactions have been treated by Jaffe and Gerace[31] and Ibarra.[32] The essence of the difficulty is the following: If single-particle states are generated in some appropriate shell-model potential, the sum of the binding energies for the transferred nucleons is, in general, not the same as the total separation energy of the transferred group of particles. Hence, the requirement of providing a correct asymptotic description of the transferred group of particles through the use of the appropriate separation energy, and a shell-model description of the individual nucleon motion, would appear to be mutually exclusive.

Fortunately, this disparity is minimal in the present treatment of the ^{42}Ca$(p, \alpha)^{39}$K reaction for

TABLE I. Calculated single-particle binding energies and wave-function expansions in harmonic-oscillator functions. The overlap of this expansion with the Woods-Saxon single-particle state is given in the last column.

Single-particle state	Binding energy (MeV) [a]	Harmonic-oscillator expansion [b] $n=0$	$n=1$	$n=2$	$n=3$	Overlap
neutron $2p_{3/2}$	5.75	−0.1916	0.9590	0.1004	0.1739	0.9968
$1f_{7/2}$	8.85	0.9608	0.2451	0.1279		0.9996
$1d_{3/2}$	16.07	0.9735	0.2093	0.0921		0.9999
proton $1f_{7/2}$	4.32 [c]	0.9571	0.2540	0.1379		0.9996
	8.62 [c]	0.9360	0.3173	0.1490		
$1d_{3/2}$	8.09	0.9815	0.1664	0.0939		0.9999
$2s_{1/2}$	9.88	−0.0957	0.9760	0.1693	0.0946	0.9994
$1d_{5/2}$	13.78	0.9744	0.2130	0.0688		0.9995

[a] Details of the Woods-Saxon well parameters for calculating these binding energies are given in the text.

[b] The harmonic-oscillator parameter had a value of 0.25 fm^{-2}.

[c] Calculated with well depths of 67 and 74 MeV, respectively.

the form factors involving the $(2p_{3/2})^2$ neutron configuration. Table II compares the experimental triton separation energy with the sum of the calculated nucleon separation energies for the various states. For the $(1f_{7/2})^2$ neutron configuration form factor however, a discrepancy of about 6 MeV exists between the calculated and experimental separation energies.

B. Three-Nucleon Form Factor

The form factor defined by Eq. (12) can be readily computed with minimal expenditure of computing time if the transformation brackets are calculated before hand and made available in tabular form. In all, values for several hundred different transformation brackets were required for all the form factor calculations.

Form factors representing a single-neutron configuration only coupled to the proton single-particle state are shown in Figs. 7 and 8. It is observed that the $(1f_{7/2})^2$ neutron configuration always results in a smaller form factor in the nuclear interior than either a $(1d_{3/2})^2$ or $(2p_{3/2})^2$ neutron configuration. The $(2p_{3/2})^2$ neutron configuration,

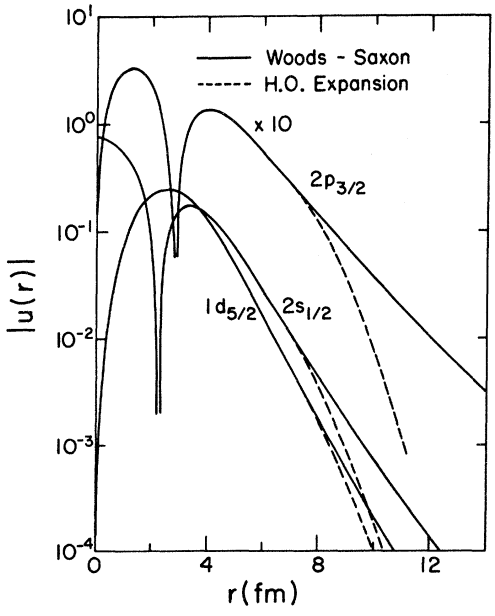

FIG. 6. Single-particle wave functions calculated in a Woods-Saxon potential well and their expansion in harmonic-oscillator (H. O.) functions. The wave functions are for a $2p_{3/2}$ neutron and $1d_{5/2}$ and $2s_{1/2}$ protons. The nuclear radius of ^{40}Ca is 4 fm.

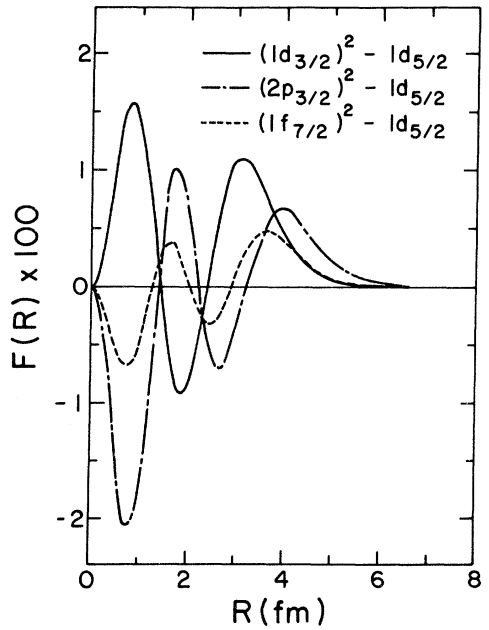

FIG. 7. Three-nucleon form factor for a $1d_{5/2}$ proton coupled to different neutron configurations. The two neutrons are coupled to a total angular momentum of zero.

TABLE II. Comparison of the experimental triton separation energy (MeV) with the sum of the nucleon binding energies for the three transferred nucleons.

State	Proton configuration	Neutron configuration $(1f_{7/2})^2$	Neutron configuration $(2p_{3/2})^2$	Experimental triton separation energy
0.0, $\frac{3}{2}^+$	$(1d_{3/2})^{-1}$	25.79	19.59	19.69
2.52, $\frac{1}{2}^+$	$(2s_{1/2})^{-1}$	27.58	21.38	22.21
5.28, $\frac{5}{2}^+$	$(1d_{5/2})^{-1}$	31.48	25.28	24.97

partly because of the lower nucleon binding energy and secondly because of the $l=1$ nucleon motion, results in a greatly increased amplitude of the form factor at large radius. A large contribution to the cross section can thus be expected even from a relatively small admixture of this component.

Sums of these "pure" form factors shown in Figs. 7 and 8 have to be made, weighted according to the two-nucleon spectroscopic amplitude in Eq. (12). Unfortunately, little reliable guidance on these two-nucleon amplitudes can be obtained from two-neutron transfer reactions. Recent analysis of the ^{42}Ca$(p, t)^{40}$Ca reaction in the neighborhood of 40-MeV proton bombarding energy by two independent groups[33,34] have led to the same conclusion. Namely, the relative magnitudes of the cross sections to the low-lying 0^+ states are very poorly predicted using presently available wave functions for ^{40}Ca and ^{42}Ca. Consequently, these two-nucleon amplitudes were treated as parameters in the DWBA calculations.

C. Optical-Model Parameters

Two sets of optical-model parameters describing the elastic scattering of protons from ^{42}Ca were used in the DWBA analysis. These are shown in the second and third rows of Table III and represent, respectively, results of optical-model analysis for $p+^{40}$Ca elastic scattering at 40.0 MeV[28] and $p+^{42}$Ca at 49.35 MeV.[35] Sensitivity of the DWBA cross sections to the proton optical parameters was not very strong, and both sets gave satisfactory results. A slight preference for the second set of parameters, since these were obtained for $p+^{42}$Ca, resulted in their adoption for all the calculations.

Much greater difficulties were encountered in finding an adequate set of $\alpha+^{39}$K optical parameters. The elastic scattering of α particles on ^{39}K, like that on ^{40}Ca, shows anomalous enhancement at backward angles[36,37] which is not well described by the conventional optical model.

Optical-model analyses of elastic α-particle scattering on ^{39}K and ^{40}Ca covering the energy range from 20–60 MeV have been performed by numerous investigators.[36-42] Without exception, it was found that only the family of potentials with $V\approx 210$ MeV gave resonable fits in the DWBA calculations. Shallower well depths in the region of $V\approx 180$ MeV yielded much inferior results. Within the $V\approx 210$ MeV family of potentials large variations in the geometrical parameters are again found[39-41] in the literature, and from these the parameter set used by Youngblood *et al.*[41] for $\alpha+^{40}$Ca was found to yield the best over-all qualitative agreement in the DWBA calculations. This set of parameters, labeled set 1 in Table III, together with slight modifications to the absorption, as represented by sets 2 and 3, were used in all the analyses.

D. DWBA Calculations

The DWBA calculations were performed using the code of Nelson and Macefield.[43] In a separate program, "pure" form factors for different neutron configurations coupled to the various proton states were calculated. A subroutine within the DWBA program then combined these "pure" form factors according to the relative neutron amplitudes, and presented the final form factor to the main DWBA routine.

The effect of varying the relative neutron amplitudes on the DWBA cross section is shown in Fig. 9 for the $\frac{3}{2}^+$ ground-state transition. Here the

TABLE III. Optical-model parameters used in the DWBA calculations for the distorted waves and the single-particle states.

Ref.			V	r	a	W	r_W	a_W	W_D[a]	V_{so}	r_{so}	a_{so}	r_c
	Single-particle states		61.8	1.152	0.692					5.90	1.014	0.526	1.32
28	$p+^{42}$Ca	set 1	44.85	1.152	0.692	4.49	1.309	0.549	3.92	4.32	1.014	0.526	1.32
35		set 2	43.6	1.16	0.78	9.80	1.32	0.54	1.9	5.80	1.03	0.59	1.25
41	$\alpha+^{39}$K	set 1	210.0	1.41	0.59	20.2	1.66	0.35					1.30
		set 2				30.0							
		set 3				25.0		0.59					

[a] The radius and diffuseness parameters for the surface term were the same as for the imaginary volume term.

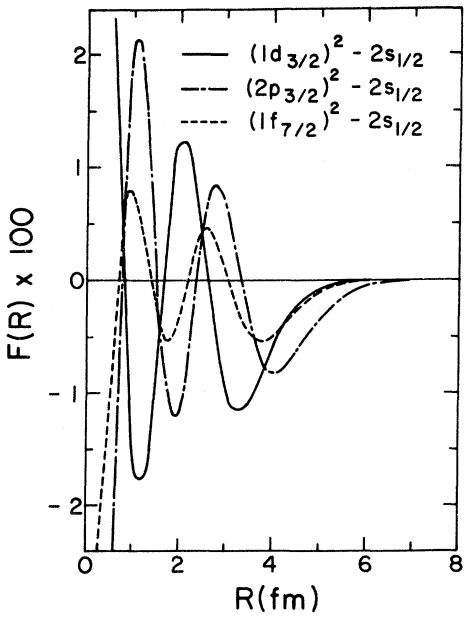

FIG. 8. Three-nucleon form factor for a $2s_{1/2}$ proton coupled to different neutron configurations. The two neutrons are coupled to a total angular momentum of zero.

$1d_{3/2}$ proton is coupled to different relative amplitudes of the $(f_{7/2})^2$ and $(p_{3/2})^2$ neutron configurations, the neutrons in each case being coupled to a total angular momentum of zero.

It is observed that the contribution of the $(p_{3/2})^2$ neutron configuration to the cross section is considerably greater than that of the $(f_{7/2})^2$ configuration, and that the latter results in little structure in the cross section. The effect of changing the relative phases between these two amplitudes is illustrated by the top and bottom curves in this figure. Strong destructive interference results when amplitudes of 1.0 and -0.5 for the $(f_{7/2})^2$ and $(p_{3/2})^2$ components, respectively, are used. Similar results for the 2.52-MeV, $\frac{1}{2}^+$ state are shown in Fig. 10. Clearly the relative magnitudes of the different neutron configurations have a pronounced effect on both the absolute magnitude of the cross section and also its shape.

Treating as parameters the neutron amplitudes and their phases, numerous calculations were performed to observe the effect on the relative cross sections to the various states and also on the qualitative shapes of the angular distributions. It was concluded that for variations of 30% in the

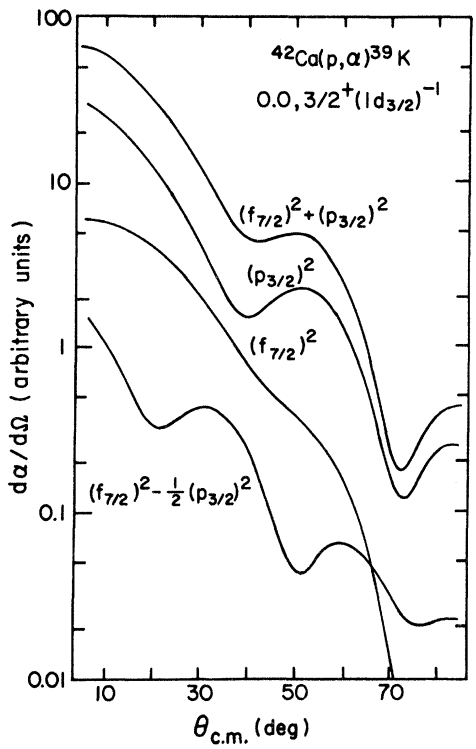

FIG. 9. DWBA cross sections for an $L=2$ transfer to the $\frac{3}{2}^+$ ground state of ^{39}K. The neutron configurations and amplitudes used in constructing the form factor are shown beside each curve. The same over-all normalization applies to all the curves.

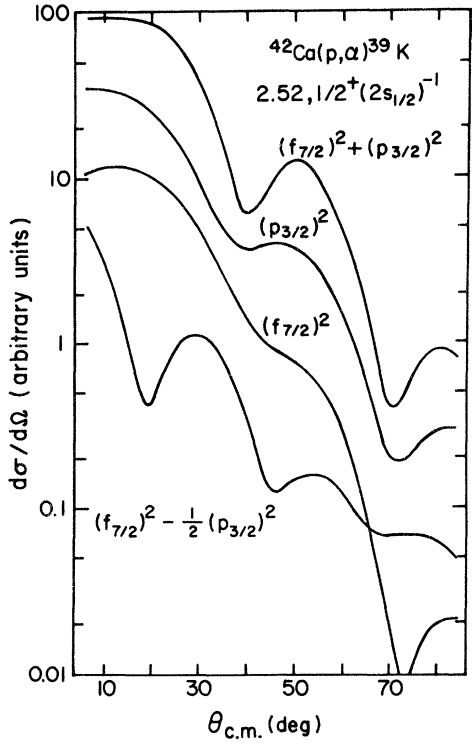

FIG. 10. DWBA cross sections for an $L=0$ transfer to the $\frac{1}{2}^+$, 2.52-MeV state in ^{39}K. The neutron configurations and amplitudes used in constructing the form factor are shown beside each curve. The same over-all normalization applies to all the curves.

TABLE IV. Summary of the optical-model parameter sets and the neutron amplitudes used to generate the different DWBA curves shown in Figs. 11 and 12. Details on the optical-model parameters are given in Table III.

Calculation	Optical-model parameters proton	α	Relative neutron amplitudes $(1d_{3/2})^2$	$(1f_{7/2})^2$	$(2p_{3/2})^2$
A	set 2	set 1	0.2	1.0	0.4
B	set 2	set 2	0.2	1.0	0.4
C	set 2	set 3	0.0	1.0	1.0
D	set 2	set 1	0.0	1.0	−0.5
E	set 2	set 1	−0.2	1.0	0.4
F	set 2	set 1	0.0	1.0	1.08

$(p_{3/2})^2$ neutron amplitude relative to the $(f_{7/2})^2$ amplitude, the relative magnitudes of the cross sections were changed very little indeed, and that the predicted shapes were equally acceptable. Furthermore, for reasonable $(d_{3/2})^2$ neutron amplitudes of the order of 0.2, the phase of this component had very little effect on the relative magnitudes of the DWBA cross sections, as will be shown later. This fact, together with the calculated two-nucleon-transfer spectroscopic amplitudes[33,34] for the ^{42}Ca$(p,t)^{40}$Ca reaction resulted in the choice of 1.0 and 0.4 for the relative amplitudes of the $(1f_{7/2})^2$ and $(2p_{3/2})^2$ neutron configurations, respectively. Proton spectroscopic information was deduced from the DWBA calculations using these neutron amplitudes. The $(d_{3/2})^2$ amplitude was permitted values of ±0.2.

DWBA fits to the angular distributions are shown in Figs. 11 and 12 for the 0.0-MeV, $\frac{3}{2}^+$, 2.52-MeV, $\frac{1}{2}^+$, 2.81-MeV, $\frac{7}{2}^-$, and 5.28-MeV $(\frac{5}{2}^+)$ states. The curves labeled A, B, C, etc., refer to calculations involving different optical-model parameters and different neutron amplitudes as indicated in Table IV.

The effect of changing the absorption in the $\alpha + {}^{39}$K optical potential is clearly seen in a comparison between curves A and B. A substantial change in the $(1p_{3/2})^2$ neutron amplitude results in only a modest change in the shape of the angular distribution (curve C, Fig. 11). Changing the relative phases of the neutron amplitudes (curve D, Fig. 12) results in a qualitatively better fit to the 5.28-MeV state, although the predicted cross section is now much too small.

From the DWBA calculations, normalized to the experimental data as shown in Figs. 11 and 12, relative proton spectroscopic factors were extracted and compared with those obtained in other proton pickup reactions. For the curves labeled A and B in these figures the results are compared

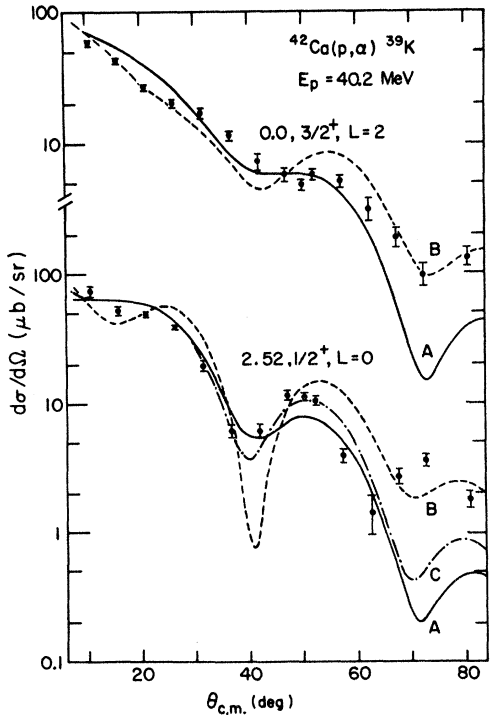

FIG. 11. DWBA fits to the (p,α) angular distributions for the 0.0- and 2.52-MeV states in ^{39}K. Parameters used in the calculations for the different curves labeled A, B, and C are given in Table IV. Each curve has been separately normalized to the data.

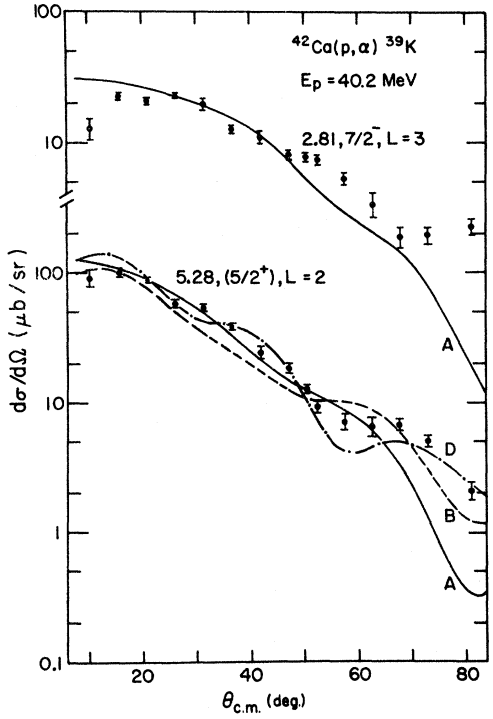

FIG. 12. DWBA fits to the (p,α) angular distributions for the 2.81- and 5.28-MeV states in ^{39}K. Parameters used in the calculations for the different curves labeled A, B, and D are given in Table IV. Each curve has been separately normalized to the data.

with the ^{40}Ca$(d, ^3$He$)^{39}$K reaction analysis as shown in Table V. The $(d, ^3$He) results were checked by recalculating the DWBA angular distributions and renormalizing to the experimental data.[21] For reasons unexplained, rather different values for the spectroscopic factors were obtained than those reported in the earlier analysis.[21] Results from these two analyses of the $(d, ^3$He) reaction are shown in the right-hand columns of Table V. The over-all normalization factor for the (p, α) DWBA cross sections was adjusted to give a value of C^2S of 3.63 for the $\frac{3}{2}^+$ ground-state transition.

With this normalization the value of C^2S for the $\frac{1}{2}^+$, 2.52-MeV state determined from the (p, α) analysis agrees surprisingly well with that from the $(d, ^3$He) analysis—1.97 to 2.35 compared with 1.70 to 1.93. This would seem to justify use of the same major neutron configurations for this transition as for the ground state. Comparing columns A and E of Table V reveals that the $(d_{3/2})^2$ neutron configuration plays a minor role since changing the phase of this component has negligible effects on the spectroscopic information.

For the $\frac{5}{2}^+$, 5.28-MeV state however, a very large value of C^2S always resulted [4 to 5 times greater than for the $(d, ^3$He) case] using the same neutron configurations as for the ground state and 2.52-MeV state. Clearly other components are also important in this transition that have not been included in the calculation. A further calculation for this state was carried out by increasing the $(2p_{3/2})^2$ neutron component as shown by calculation F in Tables IV and V. This results in a reduction of C^2S to a value of 1.93, comparable to that obtained from $(d, ^3$He). Unfortunately, the structure of these states is not well known and the above consideration may be largely speculative.

The calculations for the $\frac{7}{2}^-$, 2.81-MeV state are complicated due to the loosely bound $f_{7/2}$ proton. Calculations with proton binding energies between 4.32 and 8.62 MeV showed surprisingly small effects on the calculated cross sections of only 10%. The higher binding energy was used to obtain the result of 1.23 for C^2S for this state as shown in Table V. Again, this value is greater than for the $(d, ^3$He) case, indicating once more that important components in the wave function may have been omitted.

VI. DISCUSSION AND CONCLUSIONS

The procedure described in this paper for generating the form factor for the treatment of (p, α) reactions has been found to lead to reasonable predictions for the shapes for DWBA angular distributions and to yield proton spectroscopic information that agrees well with $(d, ^3$He) predictions for cases where the (p, α) analysis should be applicable. Ratios of these proton spectroscopic factors for the ground state and first excited state in ^{39}K, which are reasonably good single-hole states, are the same from the (p, α) and $(d, ^3$He) analysis, within the usual uncertainties expected in such analyses.

It is also clear from the (p, α) analysis that this reaction is also sensitive to components in the wave functions of the nuclei involved that are not probed by the $(d, ^3$He) reaction. No other explanation is sufficient to account for the very strong excitation of the $\frac{5}{2}^+$ states in the (p, α) reaction.

A number of effects that are likely of importance in the (p, α) reaction as well as in other direct reactions have been ignored in this study. These are the assumption of a zero-range interaction and neglect of the nonlocal nature of the interactions of the proton and α particle with the scattering nuclei. Although the former effect was not subjected to examination, several calculations were done to study the effect of using equivalent local potentials rather than nonlocal ones. Calculations of DWBA cross sections with nonlocality

TABLE V. Comparison of proton spectroscopic information (C^2S) from the (p, α) and $(d, ^3$He) reactions leading to states in the same final nucleus, ^{39}K. Results are presented for different calculations labeled, A, B, E, and F as described in Table IV.

State	Proton config.	^{42}Ca$(p, \alpha)^{39}$K A	B	E	F	^{40}Ca$(d, ^3$He$)^{39}$K Recalculated [a]	Oak Ridge [b]
0.0, $\frac{3}{2}^+$	$(1d_{3/2})^{-1}$	3.63 [c]	3.63 [c]	3.63 [c]		3.63	4.98
2.52, $\frac{1}{2}^+$	$(2s_{1/2})^{-1}$	1.97	2.35	2.01		1.70	1.93
2.81, $\frac{7}{2}^-$	$(1f_{7/2})^1$	1.23		1.28		0.58	0.50
5.28, $\frac{5}{2}^+$	$(1d_{5/2})^{-1}$	6.42	6.59	6.79	1.93	1.77	1.33

[a] Recalculated DWBA fits, renormalized to the Oak Ridge data (Ref. 21).

[b] Results from Ref. 21.

[c] The over-all normalization factor for the DWBA cross sections was arbitrarily selected to give a value of 3.63 for the ground-state transition.

parameters of 0.85 and 0.22 fm for nucleons and α particles, respectively, did not show any dramatic changes in the shapes of the angular distributions. Furthermore, the relative spectroscopic factors were very similar to those obtained without corrections for nonlocal effects.

Another aspect which complicated further interpretation of the (p, α) results was the notable lack of structure in the angular distributions. Part of the reason for this is likely the poor angular momentum matching that results in (p, α) reactions because of their generally small Q value. This requires contributions to the DWBA amplitude from the nuclear interior.

---

*Work supported in part by the Atomic Energy Control Board of Canada.

[1]K. Bethge, Annu. Rev. Nucl. Sci. 20, 255 (1970); H. H. Gutbrod, H. Yoshida, and R. Bock, Nucl. Phys. A165, 240 (1972); R. M. DeVries, Phys. Rev. Lett. 30, 666 (1973); and other recent publications.

[2]B. F. Bayman, ANL Report No. ANL-6878, 335, 1964 (unpublished), Vol. II.

[3]L. S. August, P. Shapiro, L. R. Cooper, and C. D. Bond, Phys. Rev. C 6, 2291 (1971).

[4]J. E. Glenn, C. D. Zafiratos, and C. S. Zaidens, Phys. Rev. Lett. 26, 328 (1971).

[5]R. Sherr, in *Conference on Direct Interactions and Nuclear Reaction Mechanisms, Padua, Italy, 1962,* edited by E. Clementel and C. Villi (Gordon and Breach, New York, 1963).

[6]B. F. Bayman, F. P. Brady, and R. Sherr, in *Proceedings of the Rutherford Jubilee International Conference, Manchester, 1961,* edited by J. B. Birks (Heywood, London, 1962).

[7]J. A. Nolen, Ph.D. thesis, Princeton University, 1965 (unpublished).

[8]C. B. Fulmer and J. B. Ball, Phys. Rev. 140, B330 (1965).

[9]B. Hird and T. Y. Li, Can. J. Phys. 46, 1273 (1968).

[10]T. Y. Li and B. Hird, Phys. Rev. 174, 1130 (1968).

[11]C. J. Kost and B. Hird, Nucl. Phys. A132, 611 (1969).

[12]S. H. Suck and W. R. Coker, Nucl. Phys. A176, 89 (1971).

[13]I. S. Towner and J. C. Hardy, Adv. Phys. 18, 401 (1969).

[14]I. Talmi, Helv. Phys. Acta 25, 185 (1952).

[15]M. Moshinsky, Nucl. Phys. 13, 104 (1959).

[16]Yu. F. Smirnov, Nucl. Phys. 27, 177 (1961).

[17]Yu. F. Smirnov, Nucl. Phys. 39, 346 (1962).

[18]W. Tobocman, *Theory of Direct Nuclear Reactions* (Oxford U. P., London, 1961).

[19]N. K. Glendenning, Phys. Rev. 137, B102 (1965).

[20]W. Teoh, University of Manitoba, private communication.

[21]J. C. Hiebert, E. Newman, and R. H. Bassel, Phys. Rev. 154, 898 (1967).

[22]S. Hinds and R. Middleton, Nucl. Phys. 84, 651 (1966).

[23]B. C. Robertson, R. D. Gill, R. A. I. Bell, J. L'Ecuyer, and H. J. Rose, Nucl. Phys. A132, 481 (1969).

[24]S. Maripuu and G. A. Hokken, Nucl. Phys. A141, 481 (1970).

[25]P. Goode and L. Zamick, Nucl. Phys. A129, 81 (1969).

[26]S. Wiktor, Phys. Lett. 40B, 181 (1972).

[27]B. C. Robertson, Can. J. Phys. 49, 3052 (1971).

[28]W. T. H. van Oers, Phys. Rev. C 3, 1550 (1971).

[29]A. K. Kerman, J. P. Svenne, and F. M. H. Villars, Phys. Rev. 147, 710 (1966).

[30]J. C. Parikh and J. P. Svenne, Phys. Rev. 174, 1343 (1968).

[31]R. L. Jaffe and W. J. Gerace, Nucl. Phys. A125, 1 (1969).

[32]R. H. Ibarra, Phys. Lett. 43B, 6 (1973).

[33]E. G. Adelberger, P. T. Debevec, G. T. Garvey, and R. Ohanian, Phys. Rev. Lett. 29, 883 (1972).

[34]J. P. Schapira, M. Chabre, Y. Dupont, and P. Martin, Phys. Rev. C 5, 1593 (1972).

[35]G. S. Mani, D. T. Jones, and D. Jacques, Nucl. Phys. A165, 384 (1971).

[36]K. A. Eberhard, Phys. Lett. 33B, 343 (1970).

[37]G. Gaul, H. Lüdecke, R. Santo, H. Schmeing, and R. Stock, Nucl. Phys. A137, 177 (1969).

[38]R. J. Peterson, Phys. Rev. 172, 1098 (1968).

[39]A. Budzanowski, A. Dudek, R. Dymarz, K. Grotowski, L. Jarczyk, H. Niewodniczanski, and A. Strzalkowski, Nucl. Phys. A126, 369 (1969).

[40]P. Gaillard, R. Bouché, L. Feuvrais, M. Gaillard, A. Guichard, M. Gusakow, J. L. Leonhardt, and J. R. Pizzi, Nucl. Phys. A131, 353 (1969).

[41]D. H. Youngblood, R. L. Kozub, J. C. Hiebert, and R. A. Kenefick, Nucl. Phys. A143, 512 (1970).

[42]B. Fernandez and J. S. Blair, Phys. Rev. C 1, 523 (1970).

[43]J. M. Nelson and B. E. F. Macefield, Atlas Program Library Report No. 17, 1969 (unpublished).